



3 4456 0358570 6

ORNL-5616

ornl

**OAK
RIDGE
NATIONAL
LABORATORY**



Metallurgical and Mechanical Properties of Thorium-Doped Ir-0.3% W Alloys

C. T. Liu
H. Inouye
A. C. Schaffhauser

OPERATED BY
UNION CARBIDE CORPORATION
FOR THE UNITED STATES
DEPARTMENT OF ENERGY

OAK RIDGE NATIONAL LABORATORY
CENTRAL RESEARCH LIBRARY
CIRCULATION SECTION
E5108 ROOM 125
LIBRARY LOAN COPY
DO NOT TRANSFER TO ANOTHER PERSON
If you wish someone else to see this
report, send in name with report and
the library will arrange a loan.

Printed in the United States of America. Available from
National Technical Information Service
U.S. Department of Commerce
5285 Port Royal Road, Springfield, Virginia 22161
NTIS price codes—Printed Copy: A03 Microfiche: A01

This report was prepared as an account of work sponsored by an agency of the United States Government. Neither the United States Government nor any agency thereof, nor any of their employees, makes any warranty, express or implied, or assumes any legal liability or responsibility for the accuracy, completeness, or usefulness of any information, apparatus, product, or process disclosed, or represents that its use would not infringe privately owned rights. Reference herein to any specific commercial product, process, or service by trade name, trademark, manufacturer, or otherwise, does not necessarily constitute or imply its endorsement, recommendation, or favoring by the United States Government or any agency thereof. The views and opinions of authors expressed herein do not necessarily state or reflect those of the United States Government or any agency thereof.

ORNL-5616
Distribution
Category UC-25

Contract No. W-7405-eng-26

Metals and Ceramics Division

**METALLURGICAL AND MECHANICAL PROPERTIES OF THORIUM-DOPED
Ir-0.3% W ALLOYS**

C. T. Liu H. Inouye A. C. Schaffhauser

Date Published: April 1980

OAK RIDGE NATIONAL LABORATORY
Oak Ridge, Tennessee 37830
operated by
UNION CARBIDE CORPORATION
for the
DEPARTMENT OF ENERGY



3 4456 0358570 6

CONTENTS

ABSTRACT	1
INTRODUCTION	1
EXPERIMENTAL PROCEDURES	2
RESULTS	3
Metallurgical Properties	3
Recrystallization and microstructure	3
Grain growth behavior	5
Melting point of thorium-doped alloys	7
Mechanical Properties	7
Tensile properties	7
Impact properties	9
Impact temperature effect	10
Grain size and heat treatment effects	11
DISCUSSION.....	13
Phase Relation of Ir-Th System.....	13
Segregation of Thorium at Grain Boundaries	13
Effect of Thorium Additions on Recrystallization and Grain Growth	14
Effect of Thorium on Grain-Boundary Fracture	14
Analysis of Impact Ductility.....	15
SUMMARY AND CONCLUSIONS	16
ACKNOWLEDGMENT	17
REFERENCES.....	17

METALLURGICAL AND MECHANICAL PROPERTIES OF THORIUM-DOPED Ir-0.3% W ALLOYS

C. T. Liu H. Inouye A. C. Schaffhauser

ABSTRACT

Metallurgical and mechanical properties of Ir-0.3% W alloys have been studied as a function of thorium concentration in the range 0 to 1000 ppm by weight. The solubility limit of thorium in Ir-0.3% W is below 30 ppm. Above this limit, the excess thorium reacts with iridium to form second-phase particles. Thorium additions raise the recrystallization temperature and effectively retard grain growth at high temperatures.

Tensile tests at 650° C show that the alloy without thorium additions (undoped alloy) fractured by grain-boundary (GB) separation, while the alloys doped with less than 500 ppm thorium failed mainly by transgranular fracture at 650° C. Intergranular fracture in the doped alloys is suppressed by GB segregation of thorium, which improves the mechanical properties of the boundary. The impact properties of the alloys were correlated with test temperature, grain size, and heat treatment. The impact ductility increases with test temperature and decreases with grain size. For a given grain size, particularly in the fine-grain size range, the thorium-doped alloys are much more ductile and resistant to GB fracture. All of these results can be correlated on the basis of stress concentration on GBs by using a dislocation pileup model.

INTRODUCTION

Ir-0.3% W alloys are used as postimpact containment claddings for radioactive fuel in thermoelectric generators that provide stable electrical power for a variety of outer planetary missions.¹ Iridium alloys were chosen for this application because of their high melting point, good high-temperature strength, oxidation resistance, and compatibility with oxide fuel forms and carbon insulation materials. Tungsten at a level of 0.3 wt % is added to improve the fabrication of unalloyed iridium. However, iridium and Ir-W alloys exhibit grain-boundary (GB) fracture with limited ductility in tensile tests at temperatures below 800° C at conventional strain rates (10^{-4} m/s) and in impact tests at temperatures to 1500° C at high velocities (>10 m/s).¹ The high-temperature impact ductility is particularly important for the space applications because the fuel cladding must survive a reentry impact at 1000 to 1350° C at a velocity of 50 to 85 m/s under accident conditions.

Intergranular fracture is a reflection of GB brittleness that is generally attributed to a segregation of harmful impurities to GBs. However, the GB fracture cannot be suppressed or eliminated by purification of iridium and Ir-W alloys through electron-beam melting² or zone refining.³ On the other hand, Liu and Inouye¹ have found that the high-temperature impact ductility of Ir-0.3% W alloys can be greatly improved by alloying with a trace amount of Th, Al, Fe, Ni, and Rh (total, approximately 210 ppm). Among the dopants, thorium is found to be the most effective in suppressing intergranular fracture. Spark-source mass spectrometric (SSMS) analysis of the fracture surface indicated that thorium tends to segregate at GBs in the doped alloys. A detailed Auger study by White et al.⁴ confirms the extensive segregation of thorium at the GBs.

In the present study, a series of Ir-0.3% W alloys was doped with thorium, the most beneficial element, ranging from 0 to 1000 ppm by weight. The effect of thorium addition on metallurgical and mechanical properties was investigated by various methods, including tensile and impact tests. Emphasis is placed on the correlation of the results with GB segregation of thorium and formation of a thorium-rich second phase.

EXPERIMENTAL PROCEDURES

Ir-0.3% W alloys with thorium concentrations listed in Table 1 were prepared by arc or electron-beam melting and drop casting into rectangular molds. Electron-beam-melted pure iridium and master alloys Ir-20% W and Ir 2% Th were used as the starting materials. The ingots were clad in molybdenum cover sheets and rolled between 850 and 1200°C in air with 10 to 25% reduction per pass. The molybdenum cover sheet was used for retaining heat and preventing excessive oxidation during rolling. The final sheets, with a thickness of 0.7 to 0.9 mm, were of good quality with only minor edge cracks. The as-fabricated sheets were cleaned electrolytically in KCN solution.

Chemical composition determined by SSMS analysis shows that thorium level correlates quite well with the nominal concentration in these alloys. The trace impurities in the alloys are low, at levels less than 50 ppm. Also, these alloys contain a relatively low concentration of interstitial impurities, with oxygen or carbon content below 15 ppm.

Annealing studies of the alloys were performed in vacuum ($<10^{-4}$ Pa) in the temperature range 800 to 2230°C. Sheet specimens were heated by radiation from an inductively heated tantalum susceptor, where the temperature was monitored by an optical pyrometer. For heat treatments at temperatures below 1500°C, the specimens were annealed in a resistant-heated vacuum furnace where temperatures were monitored by a Pt vs Pt-10% Rh thermocouple. Microstructures of aged specimens were examined metallographically. The polished specimens were etched electrolytically in a solution of 20 ml of HCl and 80 ml of H₂O saturated with NaCl.

Tensile testing was done on an Instron testing machine at a crosshead speed of 0.25 cm/min. Tensile specimens with a gage section 0.318 cm wide by 1.3 cm long were blanked from the alloy sheets. The specimens were ground to reduce the thickness to 0.64 mm, then annealed for 1 h at 1500°C to provide a fully recrystallized microstructure. To perform the tensile tests at elevated temperatures, a water-cooled quartz-tube vacuum system was attached to the Instron testing machine, and specimens were heated inductively in a tantalum susceptor. The load-time curves were used to generate the stress-strain data. Fracture surfaces of selected specimens were examined with a JSM-U3 scanning electron microscope (SEM) operated at 25 kV.

The uniaxial tensile impact tests were performed using impact testing equipment consisting of an environmentally controlled impact chamber and a 7.62-cm-diam gas gun to accelerate the projectile (bullet) at velocities to 85 m/s. Figure 1 shows the arrangement of specimens for impact testing. The impact specimens were loaded between two molybdenum alloy (TZM) pull rods and an end plate. The specimens were heated by radiation from an inductively heated tantalum susceptor, and the temperature was monitored by a Pt vs Pt-10% Rh thermocouple centrally located on the specimen. When the

Table 1. Thorium concentration and chemical analysis of Ir-0.3% W alloys

Nominal Th content (ppm)	SSMS analysis (ppm)										
	Al	Cu	Fe	Mo	P	Pt	Rh	S	Si	Th	W
0	5	1	5	3			20		5	<0.1	3000
30	20	30	30	10	1	5	5	3	5	30	4000
50	1	5	10	3	<1	1	20	1	10	40	2300
100	3	3	3	10	<0.3	30	10	3	<3	100	2800
200	1	30	1	3	<0.1	50	10	0.3	<1	190	2000
500	1	1	10	30	<0.3	30	50	3	<3	490	3500
1000	20	30	30	10	1	10	50	3	5	1200	4000

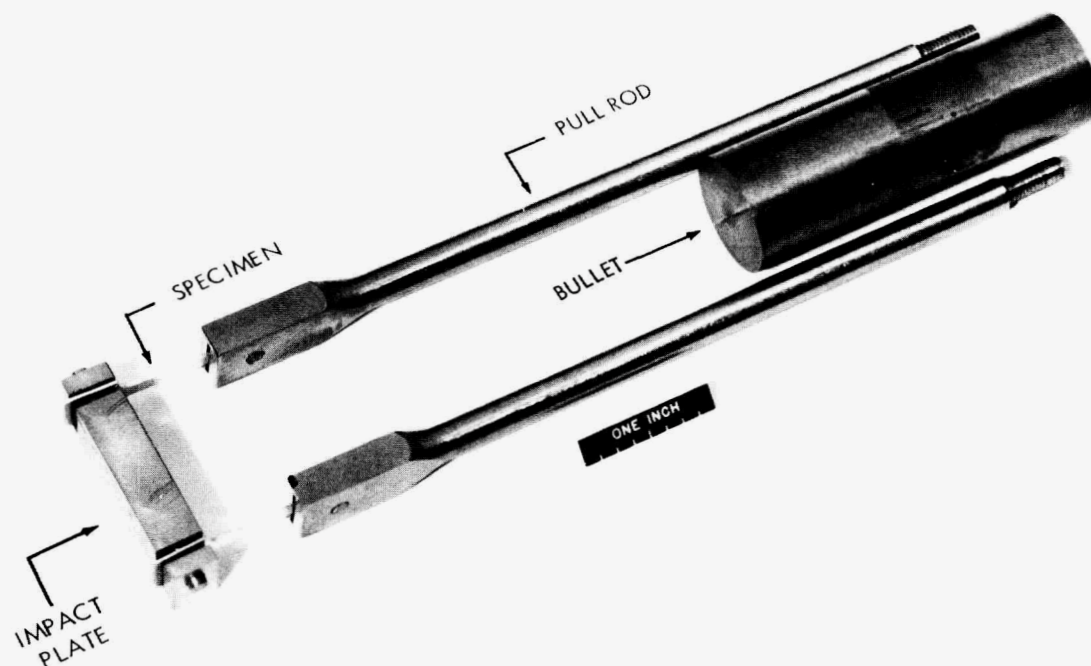


Fig. 1. Arrangement of sheet specimens for uniaxial impact test. Reduced 7%.

specimens were heated to the desired temperature, the air-driven projectile was fired at a known velocity to break the specimens. The impact elongation and the fracture mode were determined from an examination of the fractured specimens.

RESULTS

Metallurgical Properties

The metallurgical properties, including recrystallization, microstructure, grain growth, and melting point, were characterized as a function of thorium concentration.

Recrystallization and microstructure

The thorium-doped alloy sheets produced by warm rolling had a fibrous microstructure. The sheet specimens were vacuum annealed for 1 h at 800 to 1600°C to study their recrystallization behavior and microstructure. The recrystallization temperatures (T_R), determined metallographically, are shown in Fig. 2 as a function of thorium concentration. Recrystallization of the undoped alloy started at 870°C and was complete after 1 h at 1050°C. The T_R of thorium-doped alloys increases with increasing thorium content to approximately 300 ppm. Further increase in thorium does not affect T_R .

Figure 3 shows the microstructures of undoped and thorium-doped Ir-0.3% W alloys after annealing 1 h at 1500°C. The undoped specimen has an equiaxed grain structure, while the doped alloys show elongated grain structures with second-phase particles within grains and along GBs. In general, the degree of grain elongation decreases with increasing annealing time and temperature. Second-phase

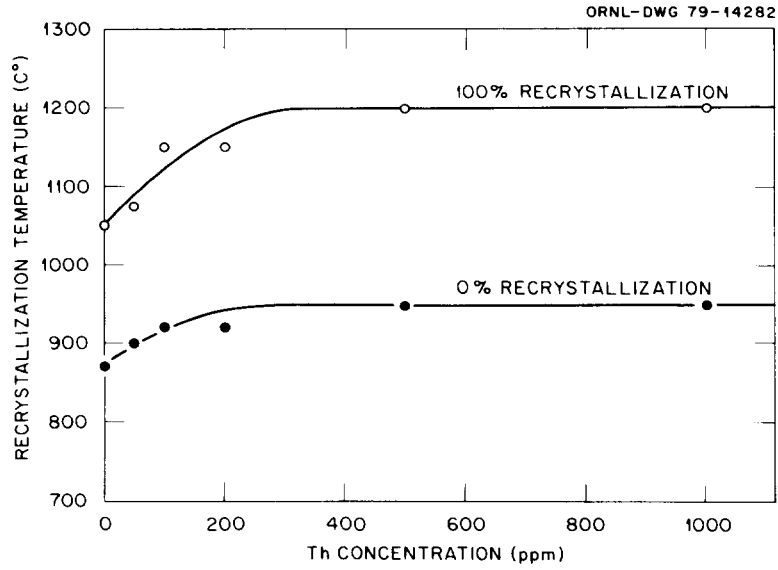


Fig. 2. Recrystallization temperature as a function of thorium concentrations in Ir-0.3% W alloys.

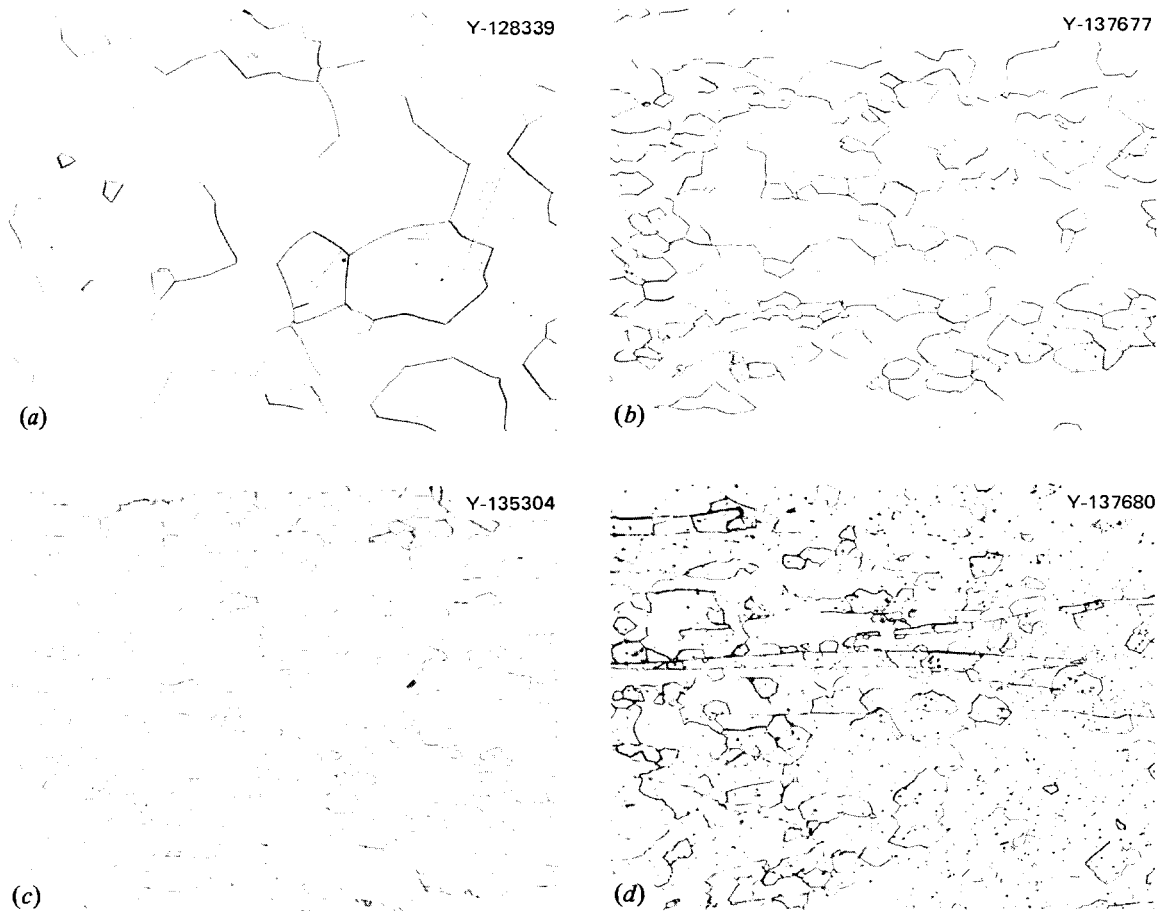


Fig. 3. Microstructures of thorium-doped Ir-0.3% W alloys annealed 1 h at 1500°C. (a) 0 ppm Th (undoped); (b) 50 ppm Th; (c) 200 ppm Th; (d) 1000 ppm Th. 100X. Reduced 4%.

particles are observed in all the doped alloys (Fig. 3). The amount of second phase increases with thorium content, and some particles appear to line up into stringers in the 1000-ppm thorium alloy (Fig. 3*d*).

The thorium distribution in doped alloys was studied by ion microprobe, using oxygen ions. The mapping of ThO_2^+ is shown in Fig. 4, where the light regions indicate the presence of thorium. The thorium is not uniformly distributed in the alloy, but is concentrated in GBs and particles. The segregation of solute thorium at GBs is revealed as networks, while the second-phase particles containing high levels of thorium appear as larger dots with high contrast in Fig. 4. The thorium-rich particles are distributed both within grains and on GBs.

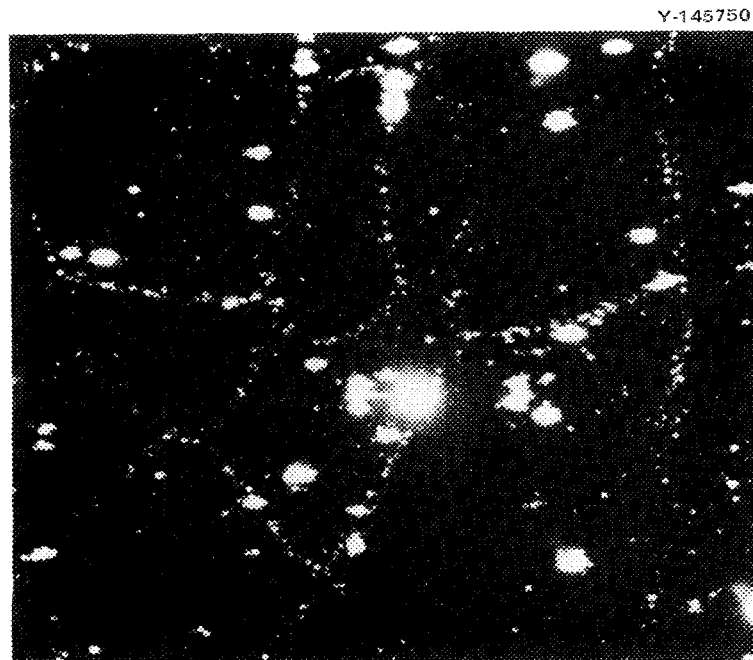


Fig. 4. Thorium distribution in the 30-ppm Th alloy, obtained by using ion microprobe. Heat treatment of the specimen: 19 h at 1500°C.

Grain growth behavior

The grain growth behavior of Ir-0.3% W alloys was determined as a function of thorium concentration. As shown in Fig. 5, thorium is very effective in retarding grain growth even at 1800°C, approximately 0.8 of the homologous temperature. The average grain diameter perpendicular to the specimen thickness was measured by the line intercept method. Figure 6 shows that the grain diameter (mean intercept length) decreases sharply with an initial increase in thorium concentration until an effective level is reached at a given heat treatment condition. Beyond the level, the grain size is almost independent of thorium concentration. The effective thorium level, as expected, increases with annealing temperature and time. For instance, the effective level is approximately 200 ppm Th for a 19-h anneal at 1500°C and increases to approximately 500 ppm for 20 h at 1800°C.

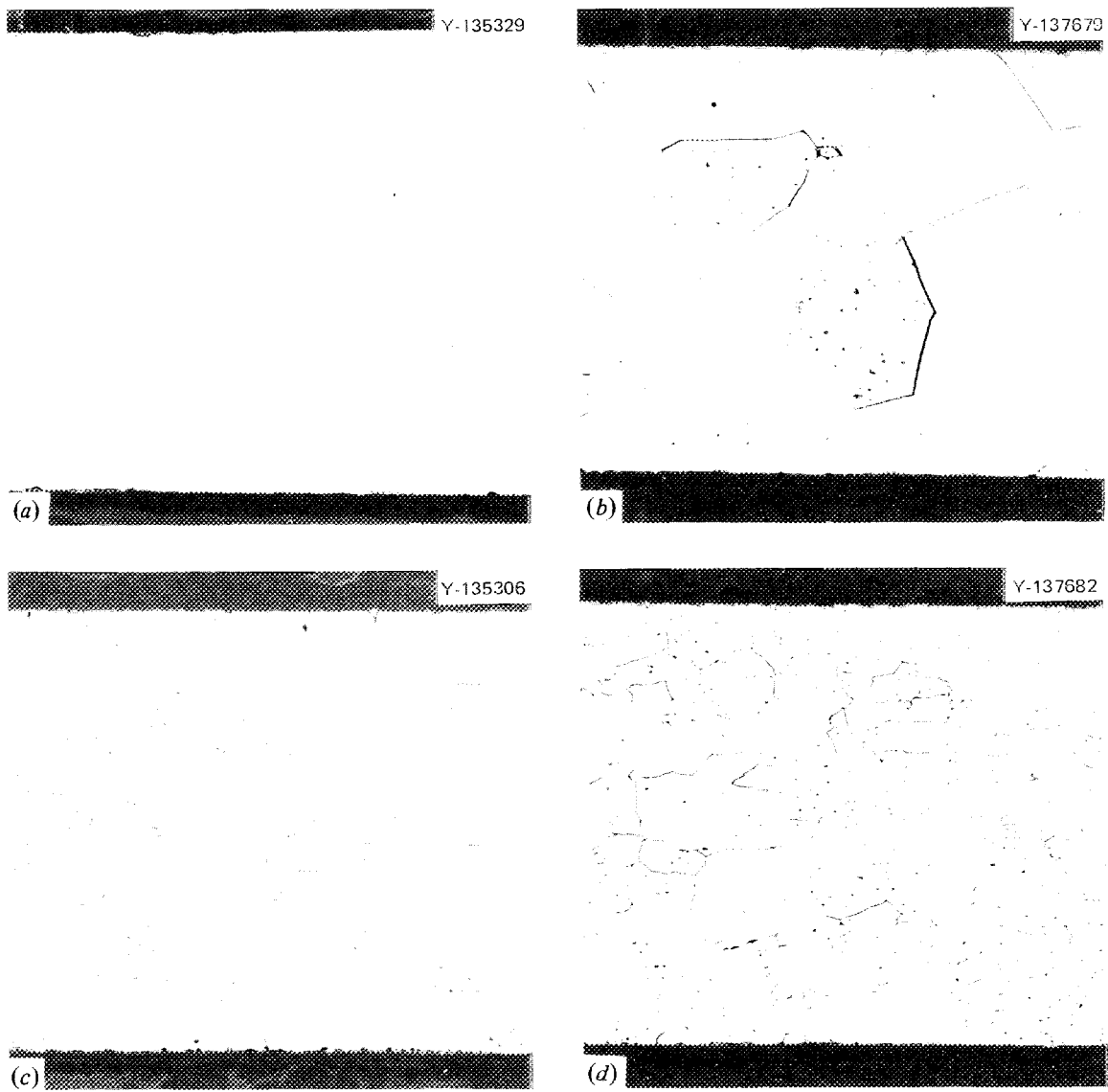


Fig. 5. Microstructures of undoped and thorium-doped Ir-0.3% W alloys annealed 1 h at 1800°C. (a) 0 ppm Th (undoped); (b) 50 ppm Th; (c) 200 ppm Th; (d) 1000 ppm Th. 100 \times . Reduced 4%.

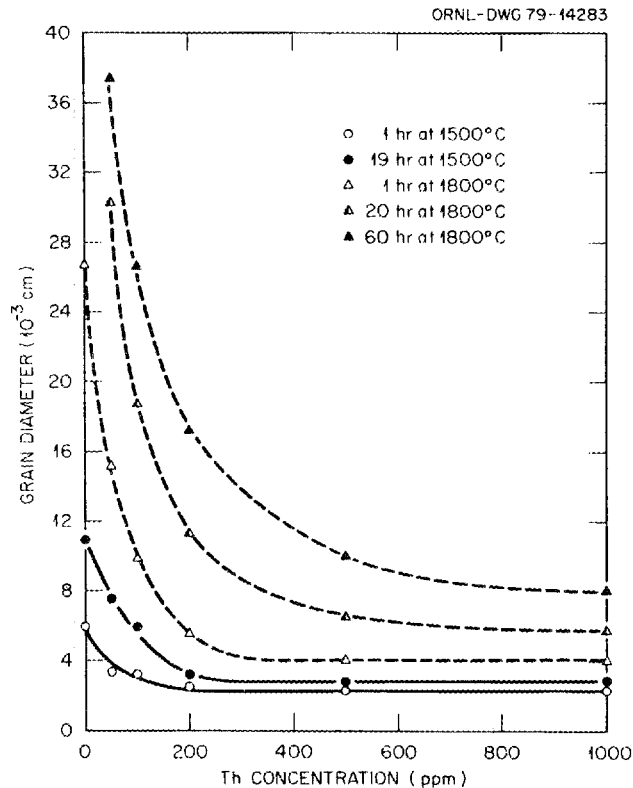


Fig. 6. Plot of grain diameter produced by various annealing treatments as a function of thorium concentration in Ir-0.3%W alloys.

Melting point of thorium-doped alloys

To determine the effect of thorium additions on the melting points of thorium-doped alloys, specimens containing 200 and 1000 ppm Th were rapidly heated to a series of temperatures up to 2230°C by inductive heating and held at temperature for 10 min. Figure 7 shows the microstructure of the heat-treated specimens, which exhibit a coarse grain structure with second-phase particles, probably ThIr_5 ,⁵ distributed within grains and on GBs. The amount of second phase on GBs appears to increase with temperature and covers most boundaries at 2200°C. Neither alloy showed any indication of incipient melting at temperatures to 2230°C, which was the limit of this test series.

Mechanical Properties

Tensile properties

Tensile properties of the thorium-doped alloys were determined at 650 and 1350°C after recrystallization for 1 h at 1500°C. The tensile data are presented in Fig. 8 as a function of thorium concentration. The yield strength increases with thorium concentration and doubles its value at a level of 200 ppm Th at 650°C. The tensile strength at 650°C also increases with thorium concentration but reaches a maximum around 500 ppm. The tensile strength is less affected by thorium at 1370°C. The alloy showed an initial increase in elongation with thorium, followed by a gradual decrease at 650°C. The peak in elongation occurred at approximately 200 ppm Th. The ductility at 1350°C is essentially insensitive to thorium concentration (Fig. 8).

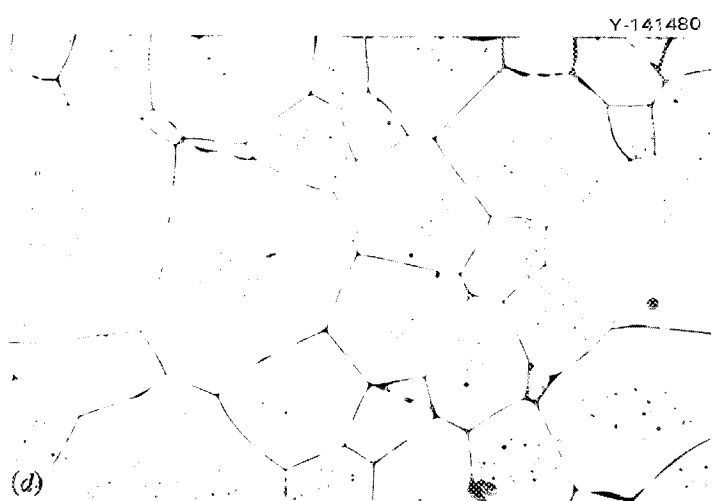
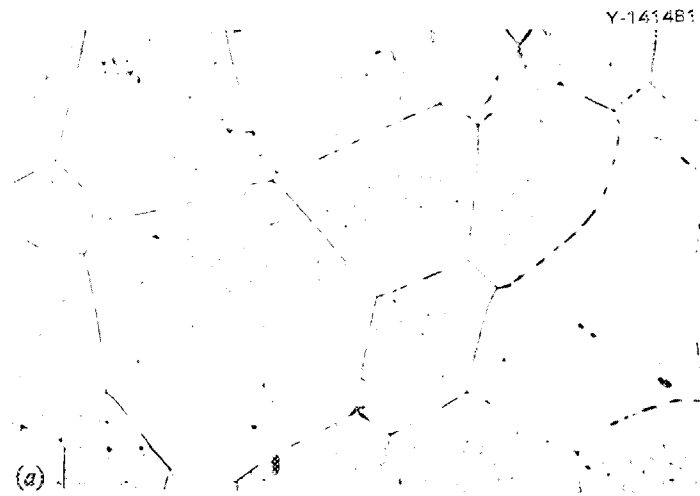


Fig. 7. Microstructures of thorium-doped Ir-0.3% W alloys subjected to 10-min heat treatment at high temperatures, 100X.
(a) 200 ppm Th, 2000°C; (b) 200 ppm Th, 2100°C; (c) 200 ppm Th, 2200°C; (d) 1000 ppm Th, 2200°C.

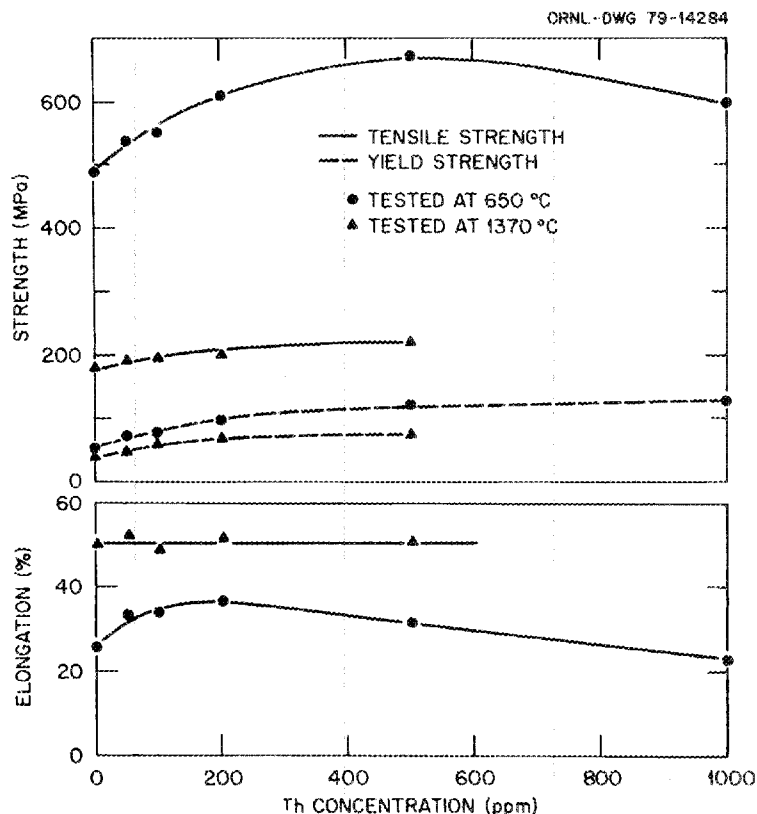


Fig. 8. Tensile properties at 650 and 1350°C as a function of thorium concentration in Ir-0.3% W alloys.

SEM examination of the tensile-fractured surface reveals that thorium additions have a dramatic effect on the fracture behavior of Ir-0.3% W alloys at 650°C. The undoped alloy fractured mainly by GB separation, as shown in Fig. 9a. The propensity for GB fracture decreases with increasing thorium concentration, and the alloy with 200 ppm Th showed mainly transgranular fracture (TF) (Fig. 9b). The TF was characterized by crystallographic steps and river patterns similar to a cleavage-type fracture generally observed in bcc metals at low temperatures. A further increase in thorium content again promotes the intergranular fracture. The alloy with 500 ppm Th failed by a mixed mode of TF and GB separation, with TF becoming more predominant in the 1000-ppm Th alloy (Fig. 9c). Discrete particles are visible at GBs and on the TF surface (Fig. 9). The particles are quite small, approximately 3 μm in the 200-ppm Th alloy annealed 1 h at 1500°C.

The brittle fracture associated with GB separation is not observed at 1350°C; instead, all alloys, whether thorium-doped or not, exhibited ductile rupture with reduction of area near 100%.

Impact Properties

Impact properties of thorium-doped Ir-0.3% W alloys were characterized as functions of test temperature, grain size, and heat treatment. All impact tests were performed at 85 m/s, the impact velocity corresponding to the maximum reentry velocity of isotopic heat sources from space. The impact results of the undoped alloy reported⁶ previously were also included here for comparison.

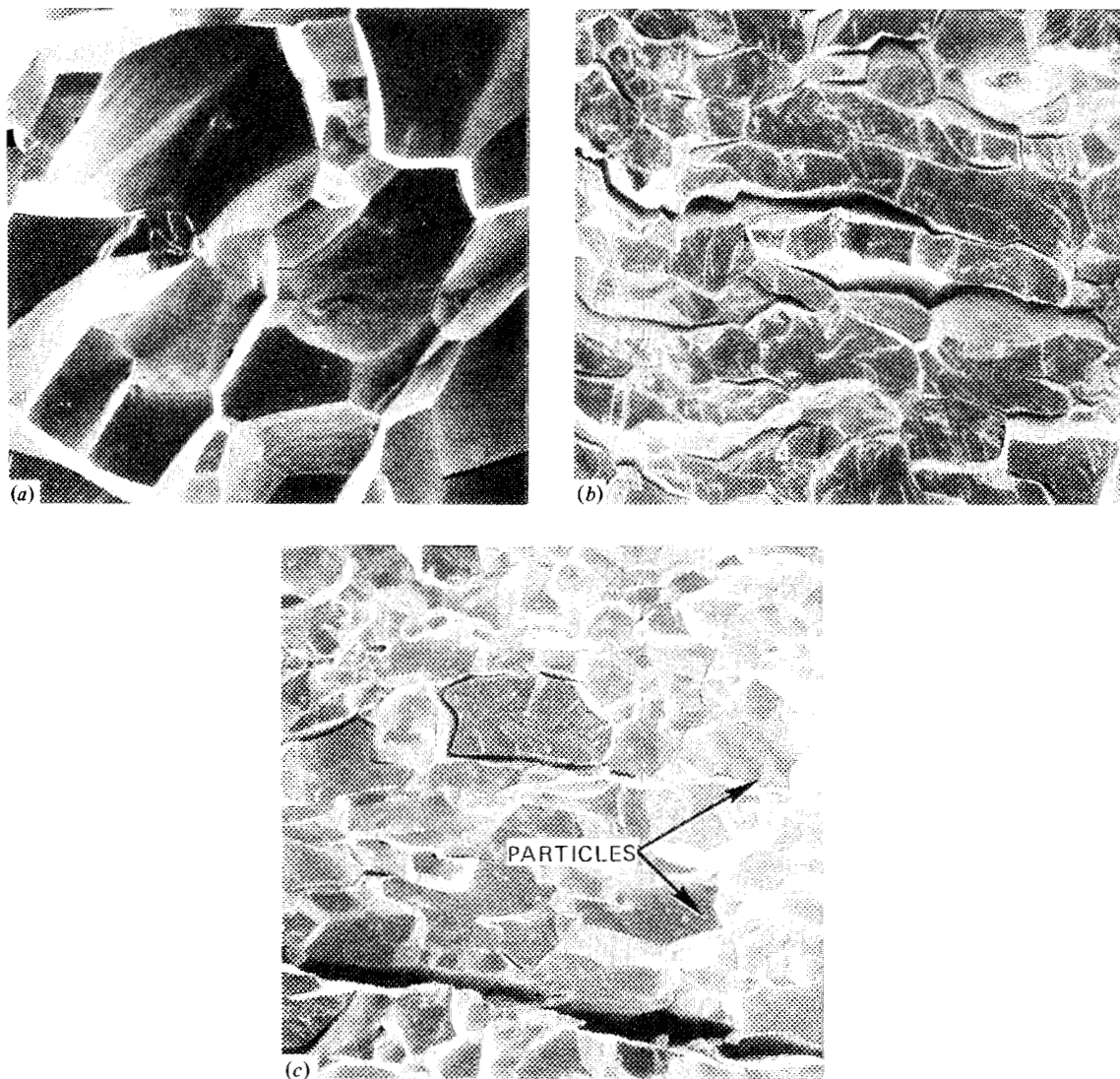


Fig. 9. SEM fractographs of Ir-0.3% W alloys fractured in tension at 650°C. 300 \times . (a) 0 ppm Th (undoped); (b) 200 ppm Th; (c) 1000 ppm Th. Reduced 18%.

Impact temperature effect

Specimens containing 200 ppm Th were heat treated for 1 h at 1500°C and impact tested to determine the effect of test temperature on impact properties. The impact elongation of both undoped and 200-ppm Th alloys increases with test temperature and becomes insensitive to temperatures above 1200°C (Fig. 10). The thorium-doped alloy is much more ductile than the undoped alloy at all test temperatures. For example, the doped alloy exhibited 29.2% elongation, while the undoped alloy showed only 5.4% at 1050°C. The undoped specimens showed GB fracture without necking at these temperatures (Fig. 11a). In contrast, the thorium-doped specimens exhibited ductile rupture (Fig. 11b) with >65% reduction of area at and above 1050°C. The fracture mode of the doped alloy changed to mixed TF and GB separation as a result of lowering the impact temperature to 950°C.

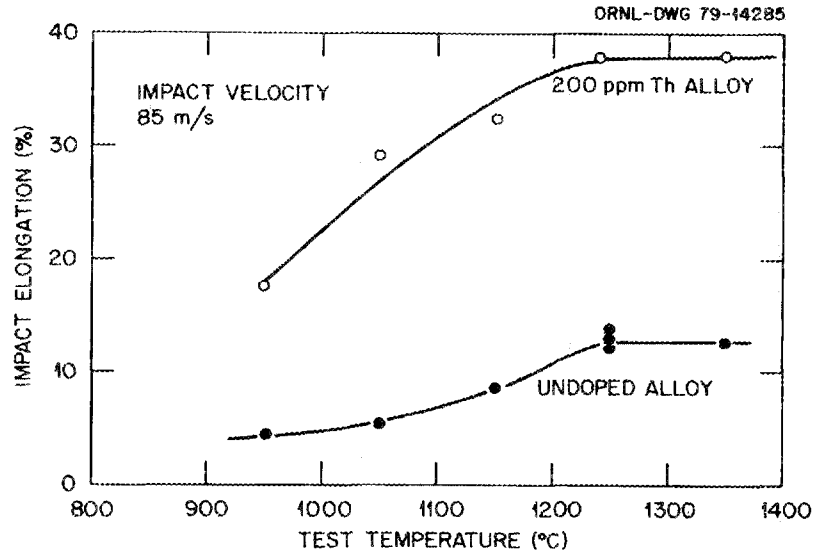


Fig. 10. Impact elongation as a function of test temperature for undoped and 200-ppm Th alloys impact tested at 85 m/s.

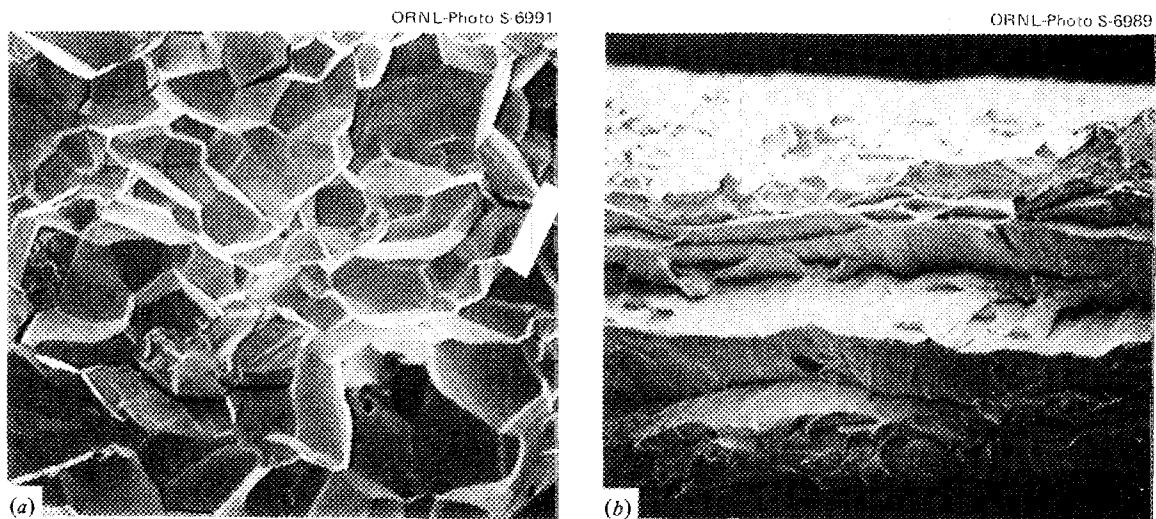


Fig. 11. SEM fractographs of Ir-0.3% W alloys impact fractured at 1050°C and 85 m/s. 200×. (a) Undoped alloy; (b) 200-ppm Th alloy. Reduced 17%.

Grain size and heat treatment effects

The impact properties of undoped and thorium-doped alloys are presented as a function of reciprocal of grain diameter* in Fig. 12 for reduction of area and in Fig. 13 for impact elongation. The variation in grain size was produced by heat treatment between 1300 to 1800°C. All the specimens were

*At a given specimen thickness, the reciprocal of grain diameter is proportional to the number of grains across the specimen.

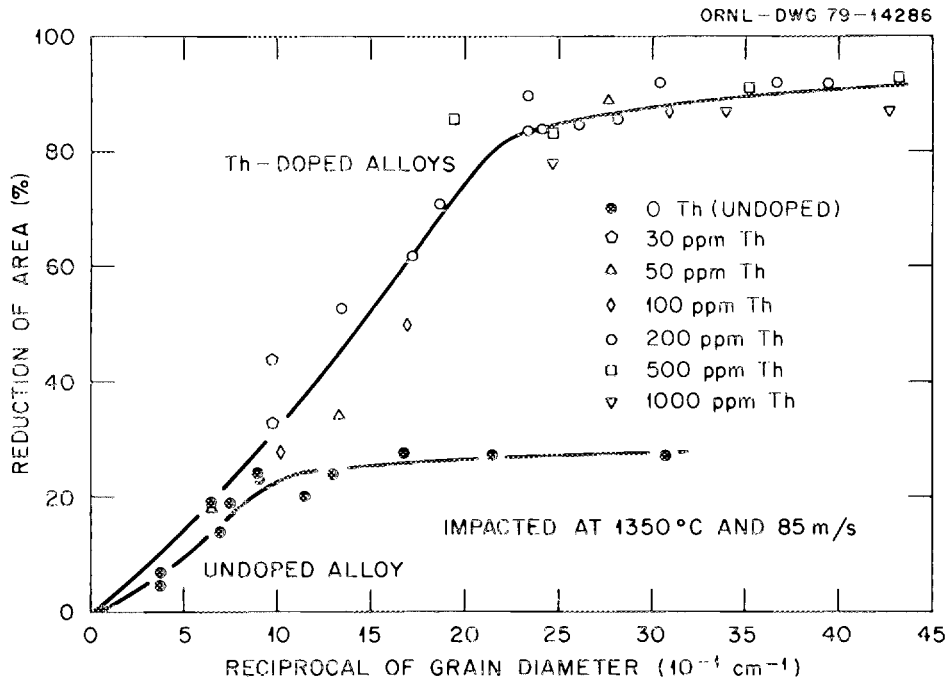


Fig. 12. Reduction of area as a function of reciprocal of grain diameter for undoped and thorium-doped Ir-0.3% W alloys impact tested at 1350°C and 85 m/s.

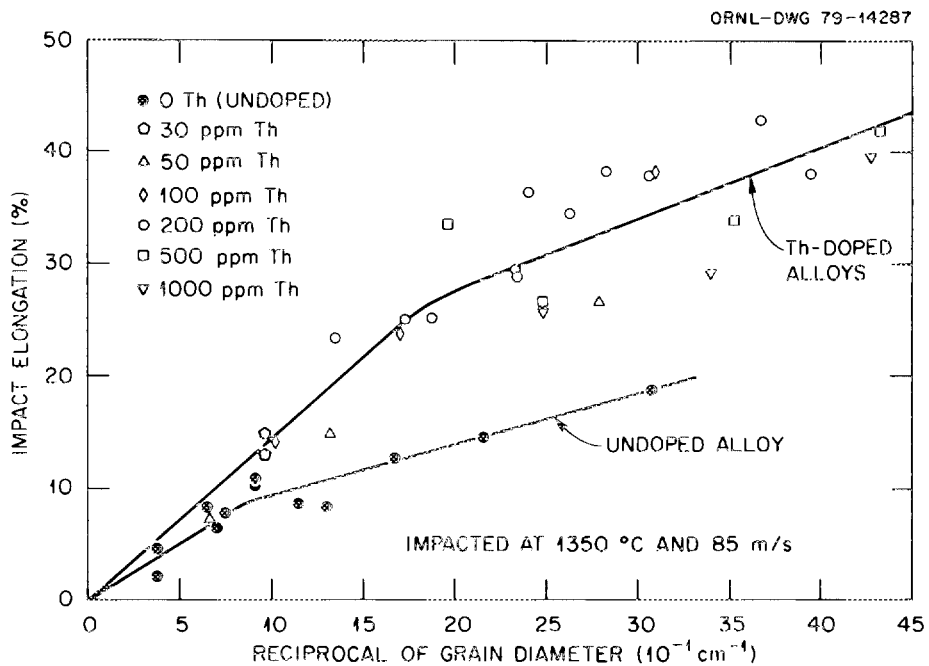


Fig. 13. Impact elongation as a function of reciprocal of grain diameter for undoped and thorium-doped alloys impact tested at 1350°C and 85 m/s.

tested under the same impact condition, that is, 85 m/s and 1350°C. The impact data of doped alloys containing 30 to 1000 ppm Th group together to fit a single curve in Figs. 12 and 13. The impact ductility is much better for doped alloys than for the undoped alloy in the fine-grain size range. For instance, at a grain size of $2.5 \mu\text{m}^{-1}$, undoped alloys had 27% reduction of area, while the doped alloys had 85% reduction of area. However, the ductility of both doped and undoped alloys decreases with increasing grain size, and the decrease becomes more dramatic in the coarse-grain size range. Both alloys appear to lose their ductility when the grain size is sufficiently coarse. This observation is in agreement with the biaxial impact results obtained recently at Los Alamos Scientific Laboratory⁷ and indicates that the beneficial effects of thorium additions on impact ductility can be offset by too coarse a grain size.

Examination of the fracture surfaces of the impact specimens with a wide range of grain sizes showed a general correlation. The specimens with more than 25% impact elongation generally fractured by ductile rupture, while those with less than 15% elongation fractured by GB separation. Between these levels the fracture mode was predominantly TF.

DISCUSSION

Phase Relation of Ir-Th System

Second-phase particles are observed in all the alloys doped with 30 to 1000 ppm Th after being annealed at 1300 to 1800°C (Figs. 3, 5, and 9). Analysis of the particles showed that they are composed of thorium (Fig. 4) and iridium.* According to the partial phase diagram of the Ir-Th system,^{5,8} the first iridium-rich compound in the diagram is of the composition ThIr₅, forming through the eutectic reaction



The observation of the second-phase particles in the doped alloys suggests that the solubility limit of thorium in iridium below the eutectic is extremely low, that is, less than the lowest concentration tested here (30 ppm). The temperature of the above eutectic reaction has been reported recently to be 2080°C by Kleykamp.⁸ However, the alloys containing 200 and 1000 ppm Th showed no indication of incipient melting at temperatures to 2230°C (Fig. 7). This indicates that the solidus or eutectic temperature of the Ir-Th alloys containing 1000 ppm is above 2230°C. Thus, alloying of iridium with thorium additions does not significantly lower the melting point of the iridium ($T_M = 2447^\circ\text{C}$). Since the solubility of thorium in iridium is very low, it is probable that the alloy with 1000 ppm Th is in the hypoeutectic composition range.† In other words, the eutectic temperature for iridium and ThIr₅ is above 2230°C.

Segregation of Thorium at Grain Boundaries

The small amount of thorium (<30 ppm) retained in solution is not uniformly distributed in the thorium-doped Ir-0.3% W alloys. Ion microprobe analysis indicates that thorium has segregated strongly to the GBs, as shown in Fig. 4. The enrichment of thorium at the GBs was first detected¹ by SSMS and then confirmed by Auger.^{4,7} White, Clausing, and Heatherly⁴ have estimated the GB concentration of thorium to be 5 to 15% in the DOP-4 type Ir-0.3% W alloy containing 30 ppm Th. Also,

*Iridium was detected in the particles by using Ir⁻ ion mapping.

†The eutectic composition has been reported to contain ~10% Th by Thomson (see ref. 5).

the thorium concentration at the GBs does not change with the bulk concentration of thorium in the alloy doped to 1000 ppm Th.⁹ Inert-ion sputtering at the fracture surface indicates that thorium is enriched only within a few atom layers of the GBs. Similar results for GB segregation of thorium in iridium have also been observed by Hecker.⁷

Since chemical analyses for thorium segregation were carried out only at room temperature, we do not know whether this is an equilibrium segregation that should occur at high temperatures. A “nonequilibrium” (such as pre-precipitation of second phase at GBs) segregation can take place during cooling of specimens from high temperature. This type of segregation is particularly favored in alloys where the solubility of solutes is low and is strongly temperature dependent. However, our impact tests indicate that adding thorium alters the fracture mode from brittle GB fracture to ductile TF at high temperatures (Fig. 11). This suppression of intergranular fracture suggests that thorium is present at the GB at temperatures at least to 1350°C. We thus believe that the GB segregation of thorium is an equilibrium type in the doped Ir-0.3% W alloys. The cause for thorium segregation is not known, but is possibly related to the large difference in atomic size of thorium and iridium.

Effect of Thorium Additions on Recrystallization and Grain Growth

The addition of thorium is very effective in raising the recrystallization temperature of doped Ir-0.3% W alloys. A previous study showed¹ that the recrystallization behavior of iridium and Ir-0.3% W alloys was sensitive to trace impurities in the ppm range. The recrystallization of pure iridium sheets produced by electron-beam melting starts at 800°C and is complete after 1 h at 950°C. However, the T_R of commercial-grade iridium containing a relatively high level of trace impurities is higher by as much as 400°C. The results shown in Fig. 2 certainly identify thorium as one of the elements that contributes to the significant increase in T_R of Ir-0.3% W.

The slower grain growth in thorium-doped Ir-0.3% W alloys can be the result of two processes. One involves the GB segregation of thorium, which retards grain growth through a solute drag mechanism.¹⁰ The second is associated with precipitation of ThIr₅ particles, which effectively pin the GB. The solubility of thorium in iridium is so low that the particles are very stable and show no appreciable growth, even at 1800°C (compare Figs. 3 and 5). This makes the particle pinning mechanism effective in both low- and high-temperature annealing treatments. At a given annealing condition, the grain diameter decreases sharply with increasing thorium content (Fig. 6) for the low-thorium alloys. This suggests that the grain size in these alloys is governed by a grain growth process that depends strongly on the amount of second-phase or thorium concentration. However, with a continuous increase in thorium content, the grain boundaries become more securely pinned due to the presence of larger amounts of second-phase particles in the matrix and at GBs. Eventually, the grain growth rate approaches zero when an effective level of thorium is reached. Beyond the level, the grain size is practically independent of thorium concentration, as shown in Fig. 6. As expected, the effective thorium level increases with both annealing temperature and time.

Effect of Thorium on Grain-Boundary Fracture

Study of fracture behavior reveals that the GBs tend to be preferred sites for failure in pure iridium and Ir-0.3% W alloy.^{1,2,11-17} The brittle fracture associated with GB separation is promoted in these materials by either a decrease in test temperature (<800°C) or an increase in strain rate. The intergranular fracture in metals is generally attributed to the segregation of harmful impurities at GBs. However, Hecker et al.¹¹ and White et al.,⁴ by using Auger electron spectroscopy, were unable to detect

impurities with significant quantity at the GBs, and they concluded that the intergranular fracture in iridium and Ir-0.3% W was intrinsic and not impurity related.

The tensile test results at 650°C indicate that the Ir-0.3% W alloys doped with <500 ppm Th failed mainly by TF rather than by GB separation (Fig. 9). Also, the doped alloys showed ductile rupture with tremendous reduction of area (except for very coarse grain size) during high-temperature impact tests. The suppression of GB fracture in the doped alloys must be due to GB segregation of thorium, which improves the mechanical properties of the boundary. Seah¹⁸ has recently proposed a theory to predict the effect of solute segregation on GB embrittlement. According to his theory, solute atoms smaller in size than those of the host element are predicted to improve the coherent strength of the GB, while the solute with larger atomic size lowers the coherent strength. Since the atomic size of thorium is larger than that of iridium by 30%, the ductilizing effect of thorium in the doped alloys does not appear to agree with Seah's prediction.

The amount of ThIr₅ particles increases with thorium content, and a part of them connect themselves into stringers in alloys containing 1000 ppm Th (Fig. 3d). The particles and stringers embrittle the GBs to a certain extent; as a result, the 1000-ppm alloy showed a mixed mode of GB separation and TF, as compared with predominantly TF in alloys containing 200 ppm Th (Fig. 9). Thus, in terms of fracture behavior, the optimum amount of thorium in Ir-0.3% W is around the 200-ppm level.

Analysis of Impact Ductility

The impact results obtained at 85 m/s indicate that the deformation and the fracture behavior of Ir-0.3% W alloys are sensitive to test temperature, grain size, and thorium addition. The GB fracture in these alloys is always promoted by decreasing test temperature or increasing grain size. In the fine-grain size range, the thorium-doped alloys are much more ductile and resistant to GB fracture than are the undoped alloys. All these results can be correlated on the basis of stress concentration on GBs, using a dislocation pileup model.⁶ Assuming that work hardening is linearly proportional to

$$\sigma = \sigma_i + k\epsilon, \quad (2)$$

impact deformation where recovery does not take place, this model predicts⁶

$$\epsilon_f = (\sigma_o - \sigma_i)/k + (\sigma_c/k)(s/d)^{1/2}, \quad (3)$$

where

- ϵ_f = fracture strain,
- σ_o = frictional stress against the motion of dislocations on slip planes,
- k, σ_i = materials constants for the stress-strain relation ($\sigma - \epsilon$) in Eq. (2),
- d = grain diameter,
- s = distance beyond the tip of a pileup,
- σ_c = cohesive strength of grain boundaries, or the critical strength required to crack grain boundaries.

At a given test condition, the above equation predicts the decrease of ϵ_f with increasing d . This is in agreement with the data correlating impact elongation with grain size (Fig. 13). Figure 14 shows a plot of impact elongation as a function of $d^{-1/2}$, as suggested by Eq. (3). A linear relation exists between ϵ_f and

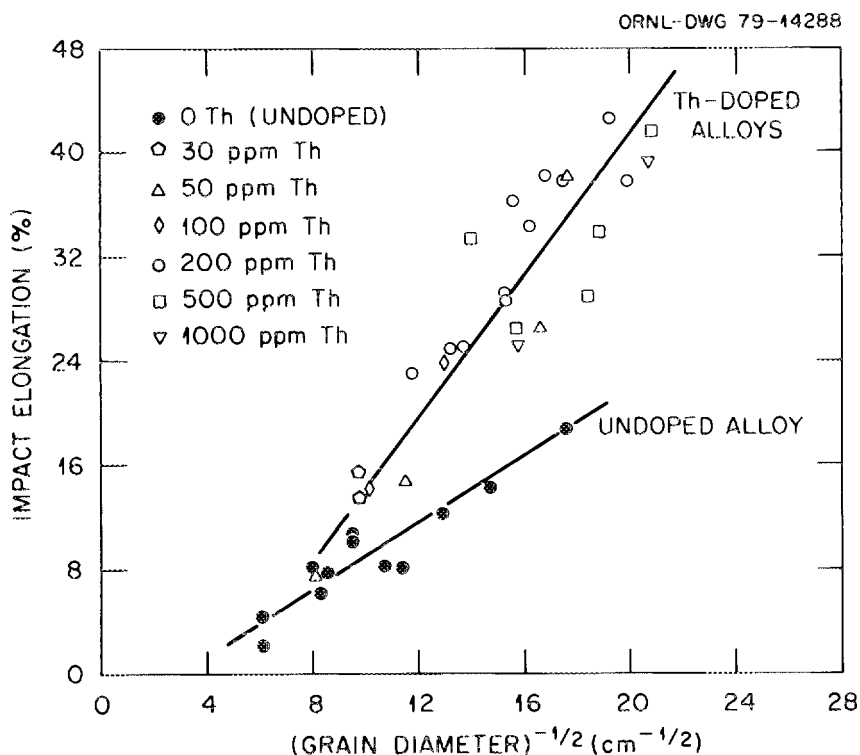


Fig. 14. Impact elongation as a function of $(\text{grain diameter})^{-1/2}$ for undoped and thorium-doped Ir-0.3% W alloys impact tested at 1350°C and 85 m/s.

$d^{-1/2}$ for the undoped alloy, which exhibited GB fracture when impact tested at 1350°C and 85 m/s. The linear relation also holds quite well for the thorium-doped alloys, even though they exhibited ductile rupture in the fine-grain size range.

According to Eq. (3), the slope of the curves in Fig. 14 determines the value of $\sigma_c(s/k)$. It is reasonable to assume that s/k is the same for the doped and undoped alloys. However, based on comparison of the slopes for the undoped and doped alloys, σ_c for the doped alloys would then have to be higher than for the undoped alloy by 110%. This certainly suggests that segregation of thorium improves the cohesive strength of the GBs. Also, thorium additions retard grain growth in the doped alloys; as a result, the doped alloys have much finer grain structures as compared with the undoped alloy under the same heat treatment conditions (Fig. 6). In Eq. (3), both the increase in σ_c and a decrease in d improve the fracture ductility. By a combination of these two effects, the impact properties of thorium-doped alloys are greatly improved.

Constants σ_i and k can be considered as yield strength and work-hardening rate of the alloys [see Eq. (3)], respectively, and both of them would be expected to increase in value with decreasing test temperature. An increase in σ_i and k should lower the impact ductility, ϵ_f , and this prediction is in accordance with the temperature effect shown in Fig. 10.

SUMMARY AND CONCLUSIONS

Ir-0.3% W alloys have been doped with thorium additions ranging from 0 to 1000 ppm for the purpose of improving their metallurgical and mechanical properties. The solubility limit of thorium in

iridium is very low, at a level below 30 ppm. Above this limit, the excessive thorium reacts with iridium to form second-phase particles with composition ThIr_5 . The thorium in solution is not uniformly distributed; instead, it segregates strongly at grain boundaries, as detected by ion microprobe and Auger analyses. The thorium-doped alloys showed no indication of incipient melting at temperatures to 2230°C , indicating that the eutectic temperature for iridium and ThIr_5 is above that temperature. Thorium additions raise the recrystallization temperature and retard grain growth at high temperatures. The grain size in low-thorium alloys is governed by the grain growth process, which depends strongly on the amount of second-phase or thorium concentration. Beyond an effective thorium level, the grain size becomes almost independent of thorium concentration.

Tensile tests indicate that thorium addition increases the strength and improves the fracture behavior of Ir-0.3% W alloys. The undoped alloy fractured by GB separation, while the alloys doped with less than 500 ppm Th failed mainly by transgranular fracture at 650°C . The suppression of the intergranular fracture in the doped alloys is due to GB segregation of thorium, which improves the mechanical properties of the boundary. The brittle fracture associated with GB separation is not observed at 1370°C ; instead, all alloys, whether thorium-doped or not, exhibited ductile rupture with reduction of area close to 100%.

The impact properties of the alloys were characterized as functions of test temperature, grain size, and heat treatment at a velocity of 85 m/s. The impact elongation of both doped and undoped alloys increases with test temperature and becomes insensitive to temperature above 1200°C . The ductility of both alloys decreases with increasing grain size, and the decrease becomes more dramatic in the coarse-grain size range. For a given grain size, particularly in the fine-grain size range, the thorium-doped alloys are much more ductile and resistant to GB fracture. All of these results can be correlated on the basis of stress concentration on GBs, using a dislocation pileup model.

ACKNOWLEDGMENT

The authors gratefully acknowledge C. O. Tarr (DOE), D. E. Harasyn (ORNL), and C. L. White (ORNL) for valuable discussions. Thanks are due to J. F. Newsome and E. H. Lee for technical assistance; to the Metals Processing Group under R. L. Heestand and D. E. Harasyn for alloy preparation and fabrication; to W. H. Christie for ion microprobe analysis; to T. J. Henson for SEM; and to W. H. Farmer for metallography.

We thank J. H. DeVan, G. M. Slaughter, S. A. David, and R. L. Heestand for reviewing the technical content of this manuscript.

REFERENCES

1. C. T. Liu and H. Inouye, *Development and Characterization of an Improved Ir-0.3% W Alloy for Space Radioisotopic Heat Sources*, ORNL-5290, (October 1977).
2. C. T. Liu and H. Inouye, *Study of Iridium and Iridium-Tungsten Alloys for Space Radioisotopic Heat Sources*, ORNL-5240, (December 1976).
3. C. T. Liu and H. Inouye, Oak Ridge National Laboratory, unpublished results.
4. C. L. White, R. E. Clausing, and L. Heatherly, to be published in *Metallurgical Transactions*, 1979.
5. J. R. Thomson, *J. Less-Common Met.* 6, 3 (1964).
6. C. T. Liu and H. Inouye, *Proceedings of the Second International Conference on Mechanical Behavior of Materials*, p. 1149-53, American Society for Metals, Cleveland, 1976.
7. S. S. Hecker, Los Alamos Scientific Laboratory, private communication.

8. H. Kleykamp, *J. Less-Common Met.* **63**, 25-33 (1979).
9. C. L. White, Oak Ridge National Laboratory, private communication.
10. D. E. Harasyn and A. C. Schaffhauser, *Grain Growth in Ir-0.3% W Alloys*, ORNL-5233, (January 1977).
11. S. S. Hecker, D. L. Rohr, and D. F. Stein, *Metall. Trans.* **9A**, 481 (1978).
12. R. N. Douglass, A. Krier, and R. I. Jaffee, *High-Temperature Properties and Alloy Behavior of the Refractory Platinum-Group Metals*, NP-10939, (August 1961).
13. R. W. Douglass and R. I. Jaffee, *Proc. ASTM* **62**, 627 (1962).
14. B. L. Mordike and C. A. Brooks, *Platinum Met. Rev.* **4**, 94 (1960).
15. F. C. Holden, R. W. Douglass, and R. I. Jaffee, p. 68 in *Symposium on New Metals*, ASTM-STP-272, 1960.
16. C. L. White and C. T. Liu, *Scr. Metall.* **12**, 727 (1978).
17. D. L. Rohr, S. S. Hecker, and L. E. Murr, p. 294 in *35th Annu. Proc., Electron Micros. Soc. Am.*, Boston, ed. G. N. Bailey, 1977.
18. M. P. Seah, *Proc. R. Soc. London, Ser. A* **349**, 534 (1976).

INTERNAL DISTRIBUTION

- | | |
|-------------------------------------|--------------------------------------|
| 1--2. Central Research Library | 27. Jar-Shyong Lin |
| 3. Document Reference Section | 28--32. C. T. Liu |
| 4--5. Laboratory Records Department | 33. J. C. Ogle |
| 6. Laboratory Records, ORNL RC | 34. N. H. Packan |
| 7. ORNL Patent Section | 35. A. E. Pasto |
| 8. R. L. Beatty | 36. P. L. Rittenhouse |
| 9. P. T. Carlson | 37. A. F. Rowcliff |
| 10. J. V. Cathcart | 38. A. C. Schaffhauser |
| 11. G. W. Clark | 39. J. E. Selle |
| 12. R. E. Clausing | 40. G. M. Slaughter |
| 13. R. G. Donnelly | 41. M. H. Yoo |
| 14. C. B. Finch | 42. G. C. Wei |
| 15. T. G. Godfrey, Jr. | 43. C. L. White |
| 16. R. J. Gray | 44. F. W. Wiffen |
| 17. D. E. Harasyn | 45. A. L. Bement, Jr. (Consultant) |
| 18. R. L. Heestand | 46. W. R. Hibbard, Jr. (Consultant) |
| 19. R. F. Hibbs | 47. E. H. Kottcamp, Jr. (Consultant) |
| 20. M. R. Hill | 48. M. J. Mayfield (Consultant) |
| 21--25. H. Inouye | 49. J. T. Stringer (Consultant) |
| 26. W. J. Lackey | |

EXTERNAL DISTRIBUTION

50. Air Force Weapons Laboratory, Kirtland Air Force Base, DYUS, Albuquerque, NM 87116
Michael Seaton
51. Battelle Columbus Laboratories, 505 King Ave., Columbus, OH 43201
E. L. Foster
- 52--53. E. I. du Pont de Nemours, Savannah River Plant, Aiken, SC 29801
R. A. Brownback
W. R. Kanne
54. E. I. du Pont de Nemours, Savannah River Laboratory, Aiken, SC 29801
R. T. Huntoon
55. Fairchild Industries, 20301, Century Blvd., Germantown, MD 20767
A. Schock
56. General Atomic Co., P.O. Box 81608, San Diego, CA 92138
N. B. Elsner
57. General Electric Co., Valley Forge Space Center, P.O. Box 8048, Philadelphia, PA 19101
C. W. Whitmore
58. Jet Propulsion Laboratory, California Institute of Technology, 4800 Oak Grove Drive,
Pasadena, CA 91103
J. E. Mondt
59. Johns Hopkins University, Applied Physics Laboratory, Johns Hopkins Road, Laurel, MD 20810
J. C. Hagan

- 60–61. Los Alamos Scientific Laboratory, P.O. Box 1663, Los Alamos, NM 87545
 S. E. Bronisz
 S. S. Hecker
62. Minnesota Mining and Manufacturing Co., St. Paul, MN 55101
 J. D. Hinderman
- 63–64. Monsanto Research Corp., P.O. Box 32, Miamisburg, OH 45342
 E. W. Johnson
 W. C. Wyder
65. Sundstrand Energy Systems, 4747 Harrison Ave., Rockford, IL 61101
 E. Krueger
66. Teledyne Energy Systems, 110 W. Timonium Rd., Timonium, MD 21093
 W. E. Osmeyer
67. DOE, Albuquerque Operations Office, P.O. Box 5400, Albuquerque, NM 87115
 D. Plymale
68. DOE, Dayton Area Office, P.O. Box 65, Miamisburg, OH 45342
 H. N. Hill
- 69–78. DOE, Division of Advanced Nuclear Systems and Projects, Washington, DC 20545
 R. C. Brouns R. B. Morrow
 F. M. Dieringer B. J. Rock
 G. L. Bennett C. O. Tarr
 N. Goldenberg N. R. Thielke
 J. S. Griffio
 J. J. Lombardo
79. DOE, Office of Energy Research, Office of Basic Energy Sciences, Washington, DC 20545
 L. C. Ianniello
- 80–81. DOE, San Francisco Operations Office, 1333 Broadway, Wells Fargo Building,
 Oakland, CA 94612
 L. Lanni
 W. L. Von Flue
82. DOE, Savannah River Operations Office, P.O. Box A, Aiken, SC 29801
 W. T. Goldston
83. DOE, Oak Ridge Operations Office, P.O. Box E, Oak Ridge, TN 37830
 Office of Assistant, Manager, Energy Research and Development
- 84–311. DOE, Technical Information Center, Office of Information Services, P.O. Box 62,
 Oak Ridge, TN 37830
 For distribution as shown in TID-4500 Distribution Category UC-25 (Materials)